Protective Fuzzy Control of a Two-Wheeled Mobile Pendulum Robot: Design and Optimization

ÁKOS ODRY, ISTVÁN KECSKÉS, ERVIN BURKUS, PÉTER ODRY
Department of Control Engineering and Information Technology
University of Dunaújváros
Táncsics Mihály út 1/A, H-2401 Dunaújváros
HUNGARY
odrya@uniduna.hu, kecskes.istvan@gmail.com, burkus@uniduna.hu, podry@uniduna.hu

Abstract: - This paper describes the design and optimization results of a cascade fuzzy control structure developed and applied for the stabilization of an underactuated two-wheeled mobile pendulum system. The proposed fuzzy control strategy applies three fuzzy logic controllers to both provide the planar motion of the plant and reduce the inner body oscillations. Among these controllers, one is a special PI-type fuzzy logic controller designed to simultaneously ensure the linear speed and prevent high current peaks in the motor drive system. The input-output ranges and membership functions of the controllers are initially selected based on earlier studies. A complex fitness function is formulated for the quantification of the overall control performance. In this fitness function, the quality of reference tracking related to the planar motion, the efficiency of the suppression of inner body oscillations as well as the magnitude of the resulting current peaks in the driving mechanism are considered. Using the defined fitness function, the optimization of the parameters of fuzzy logic controllers is realized with the aid of particle swarm optimization, yielding the optimal possible control performance. Results demonstrate that the optimized fuzzy control strategy provides satisfying overall control quality with both fast closed loop behavior and small current peaks in the driving mechanism of the plant. The flexibility of the proposed fuzzy control strategy allows to protect the plant's electro-mechanical parts against jerks and vibrations along with smaller energy consumption. At the end of the paper, a look-up table based implementation technique of fuzzy logic controllers is described, which requires small computational time and is suitable for small embedded processors.

Key-Words: - fuzzy tuning, particle swarm optimization, inverted pendulum robot, robot control

1 Introduction

Fuzzy logic provides an easy, expert oriented way to establish control structures. The fuzzy inference can be defined with heuristic IF-THEN rules which are collected based on both the observations related to system dynamics and human common sense [1]. This approximate reasoning allows to cover model imprecision and uncertainties, moreover, the broadly defined fuzzy sets yield robust and smooth control action which in many cases provides superior control performance compared to linear solutions [2]-[6].

Although, the heuristically defined inference machine roughly meets the design requirements it usually provides a suboptimal control performance. This suboptimal control performance can be further improved by trial and error tuning. However, the engineering intuition based iterative tuning becomes rather difficult if complex nonlinear systems with high order dynamics are controlled. Moreover, this way the best control performance cannot be guaranteed. The tuning procedure can be realized with numerical optimization as well, which replaces the designer's tedious, iterative task and optimizes the control parameters by locating the minimum of the formulated fitness function.

This paper introduces a flexible fuzzy control structure and describes its optimization procedure realized with the aid of particle swarm optimization (PSO). The investigated control structure was originally developed with empirical rules and trial and error tuned membership functions for the stabilization of a naturally unstable mechatronic system, a so-called mobile wheeled pendulum (MWP) [7], [8].

Two solutions are proposed to enhance the initial control performance. On one hand, a special PI-type fuzzy logic controller (FLC) is applied in the control structure which both ensures fast reference tracking and reduces the current peaks in the motor drive system. This PI-type FLC allows to protect the electro-mechanical parts of the plant, moreover, it

provides fast closed loop behavior. On the other hand, the optimization procedure of the proposed fuzzy control structure is outlined, yielding the optimal possible overall control performance.

The mechatronic system is composed of two coaxial wheels (no additional caster), and an inner body (hereinafter IB) that forms a pendulum between the wheels, as illustrated in Fig. 1. Since the system has only two contact points with the supporting surface, the IB tends to oscillate when the wheels are actuated. This motion leads to a control challenging problem, which is the simultaneous stabilization of the IB and the predefined control of the planar motion of the wheels.

Linear controllers had been elaborated and analyzed for this type of systems in [9]-[11]. However, the design of the controllers was based on trial and error procedures and the achievable control performance has not been investigated, which motivates this study.

The electro-mechanical properties of the system along with its mathematical model were described in detail in [12]. A fuzzy logic based anti-sway speed control structure was elaborated in [13], where simulation and implementation results showed that the proposed controllers successfully ensured both the planar motion and the stabilization of the IB. This fuzzy inference machine was characterized by heuristically defined membership functions and IF-THEN rules collected from observations of the system dynamics. Moreover, the control performance achieved with the preceding fuzzy control structure was analyzed by evaluating different error integrals and transient responses. The study in [2] compared the fuzzy anti-sway speed control structure with a linear-quadratic-Gaussian (LQG) controller elaborated in [3]. The measurement results related to the real system dynamics showed that the proposed fuzzy control structure provided better overall control performance, however, the LQG control strategy showed faster system dynamics for transient events. A video demonstration of the closed loop behavior is available on the website [14].

In [15] a control performance enhancement procedure was proposed. The optimal possible FLC parameters were found based on both the definition of an objective (or fitness) function for control quality evaluation and utilization of the PSO algorithm on the parameters of the fuzzy inference machine. These parameters were related to the

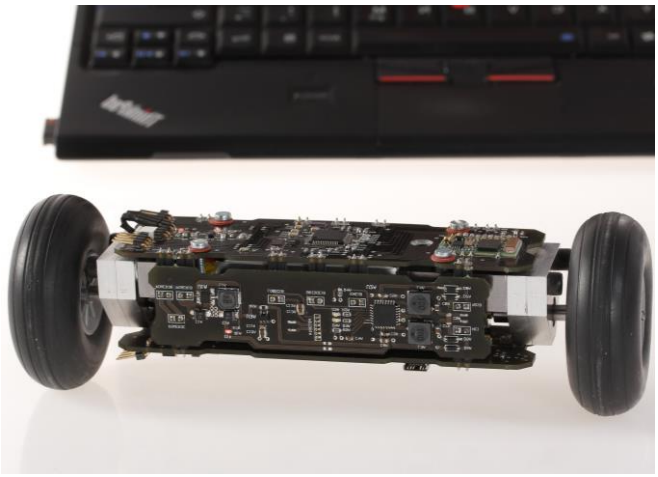

Fig. 1. Photograph of the mobile pendulum system.

input-output ranges and the shapes of membership functions. The fitness function used in the optimization was formulated such a way to make the optimized fuzzy control structure provide fast system dynamics as well as reduce the IB oscillations.

The goal of this paper is to present a protective fuzzy logic based control strategy for plants that highly require vibrations and jerks to be reduced in their electro-mechanical parts [16], [17]. Moreover, this paper investigates and measures the achievable control performance through the application of numerical optimization. The paper provides the interested reader an example of how to elaborate an optimization procedure of control structures developed for mechatronic systems.

The rest of this paper is organized as follows. Section 2 introduces the mechatronic system and its nonlinear mathematical model. In section 3 the fuzzy anti-sway speed control structure is discussed. Section 4 introduces the optimization method, formulates a complex fitness function and discusses the optimization results. In section 5, a look-up table based implementation of the FLC controllers is described. Finally, section 6 contains the conclusions and the future work recommendations.

2 Mechatronic system

2.1 Electro-mechanical properties

The mechanical structure of the MWP consists of two coaxial wheels and a steel IB. As it can be seen in Fig. 1, no caster wheel is attached to the body, therefore the MWP has only two contact points with

the supporting surface. The wheels are actuated through DC motors that form the connection between the electrical and mechanical sides. The motors are attached to-, while the embedded electronic parts are placed around the IB. The torque produced by the motors is transferred to the wheels through rolling bearings [12].

The embedded electronics is built around two 16-bit ultra-low-power Texas Instruments microcontrollers. The system dynamics is measured with three-dimensional MEMS accelerometers and gyroscopes as well as incremental encoders are attached to the shafts of the motors. The DC motors are driven through H-bridges with pulse width modulation (PWM) signals [18]. The embedded electronics also contains a wireless communication module that enables the recording of the measurement results [3].

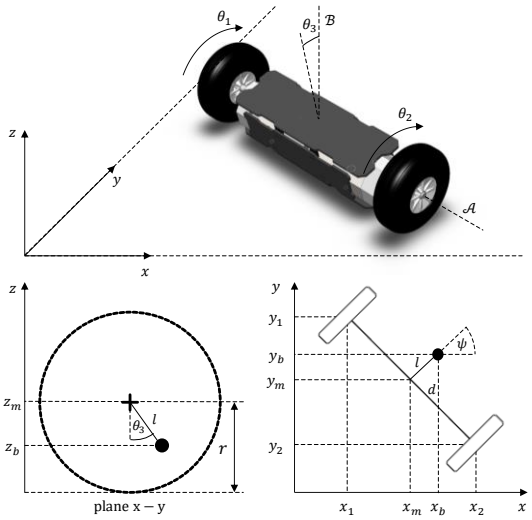

Fig. 2. Plane and side view of the MWP and its spatial coordinates.

2.2 Mathematical model

The simulation environment consists of the mathematical model of the plant and the control structure, forming together the closed loop. The mathematical model has been derived in an earlier study [12], the main parameters are depicted in Fig. 2. The angular positions of the wheels are denoted with θ_1 and θ_2, while θ_3 indicates the oscillation angle of the IB. The distance between the center of mass of the IB and the wheel axis is marked with l, moreover, the radius of the wheels and the distance between them are denoted with r and d, respectively.

The nonlinear state-space representation $\dot{x}(t) = h(x,u)$ of the MWP dynamics is described as [12]:

$$\dot{x}(t) = \begin{bmatrix} \dot{q} \\ M(q)^{-1}\left(\tau_a - \tau_f - V(q,\dot{q})\right) \\ \frac{1}{L}\left(u - k_E k \begin{bmatrix} 1 & 0 & -1 \\ 0 & 1 & -1 \end{bmatrix} \dot{q} - RI\right) \end{bmatrix}, \qquad (1)$$

$$y(t) = Cx(t),$$

where $x_{8\times1} = (q, \dot{q}, I)^T$ is the state vector, $q_{3\times1} = (\theta_1, \theta_2, \theta_3)^T$ contains the configuration variables, while $I_{2\times1} = (I_1, I_2)^T$ and $u_{2\times1} = (u_1, u_2)^T$ denote the currents and voltages of the motors, respectively. Moreover, $M(q)$ is the 3-by 3 inertia matrix and $V(q, \dot{q})$ is the 3-dimensional vector term including the Coriolis, centrifugal and potential force terms, while τ_a and τ_f indicate the torques transmitted to the wheels and the effect of friction. The applied DC motors are characterized by the rotor resistance R and inductance L, the back-EMF constant k_E, and additionally the ratio of the gearbox k. The output matrix C of the state space equation is selected such a way to produce the $y_{5\times1} = (v, \theta_3, \omega_3, \xi, I_{avg})$ output, where $v = r(\theta_1 + \theta_2)/2$ is the linear speed of the plant, $\omega_3 = \dot{\theta}_3$ is the oscillation rate of the IB, while $\xi = r(\dot{\theta}_2 - \dot{\theta}_1)/d$ and $I_{avg} = (I_1 + I_2)/2$ denote the yaw rate and the average motor current, respectively.

3 Control solutions

The objective of the employed control structure is to simultaneously ensure the planar motion of the MWP and suppress the resulting IB oscillations, jerks and current peaks (so-called anti-sway speed control of the plant). The design requirements are summarized with the following control objectives:

- $\lim_{t\to\infty} v(t) = v_d$ for the linear speed,
- $\lim_{t\to\infty} \xi(t) = \xi_d$ for the yaw rate,
- $\lim_{t\to\infty} \omega_3(t) = 0$ for the IB stabilization,
- with minimized $\dot{I}_A$ (current peaks),

where v_d and ξ_d denote the desired linear speed and yaw rate values.

The simulation of the closed loop behavior was performed in MATLAB/Simulink environment. The continuous-time state space equation (1) was implemented using an S-function block, while the FLCs were realized with the *Fuzzy Logic Toolbox* of MATLAB. In the simulation model discrete-time controllers were implemented, therefore a $T_s = 0.01$ sec sampling time was also considered, which

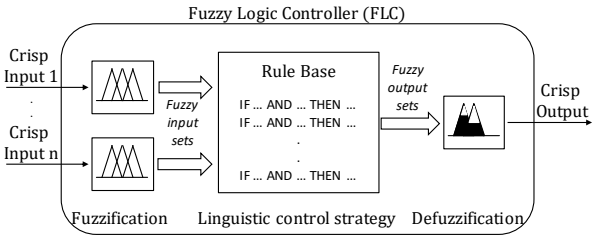

Fig. 3. Structure of the fuzzy logic controller.

equals to the sampling time of the accelerometer and gyroscope sensors on the MWP.

3.1 Fuzzy control structure

The inference mechanism of fuzzy control is based on the application of fuzzy sets. This allows to introduce linguistic variables (such as *small* and *large* for reasoning about the current consumption) and associate them with membership functions [1]. The block diagram of a fuzzy logic controller (FLC) is depicted in Fig. 3, where three main parts are identified as follows.

- The fuzzification block converts the continuous variables to linguistic variables.
- The control strategy is described with a rule base that maps the inputs to output linguistic variables representing the control signals.
- The aggregation of output linguistic variables is mapped into a real number (crisp control signal) through the defuzzification block.

A fuzzy control structure that stabilizes the MWP was originally developed in [2], [13]. Inspired by the results of [17], this paper introduces a protective PI-type FLC and applies it in the aforementioned control structure. The protective PI-type FLC allows to significantly reduce the jerks and current peaks in the electro-mechanical parts of the MWP. Since, the control structure was described in earlier studies in detail, the emphasis is on the description of the protective PI-type FLC.

The modified control structure consisting of three cascade-connected FLCs is depicted in Fig. 4. FLC1 and FLC3 are responsible for the control of linear speed and yaw rate of the plant (planar motion), respectively, while FLC2 is applied for the suppression of the IB oscillations. The membership functions and rule bases of FLC2-3 are described in detail in [2]. The inputs of the PD-type FLC2 are the oscillation error e_{θ_3} and its time derivative e_{ω_3}, while the output signal is denoted with u_{θ_3}. FLC3 is a PI-type controller whose input is the yaw rate

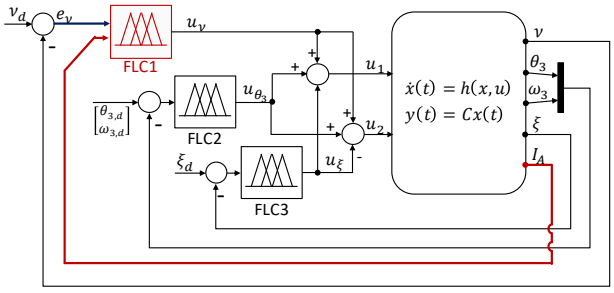

Fig. 4. Block diagram of the control structure.

error $e_\xi = \xi_d - \xi$, while u_ξ indicates its control signal.

The protective PI-type fuzzy logic controller is denoted with FLC1 (red block in Fig. 4) and its structure is shown in Fig. 5a. The task of this controller is to both ensure the MWP's linear speed and reduce the current peaks in the motor drive system. Therefore, the linear speed error $e_v = v_d - v$ and the average motor current I_A form the inputs of the controller. The control signal is denoted with u_v and is a combination of the crisp proportional and integral tags (first and second outputs of the FLC, see Fig. 5a). The rule base was defined considering the following facts:

- IF the speed error is positive (negative), THEN positive (negative) control action is applied, however,
- IF in the same time the motor current is large, THEN the aforementioned control action is decreased with negative (positive) protective voltage to reduce the current peak.

These deductions were expanded into six rules given in Table 1. Three membership functions were chosen to describe the speed error with the fuzzy sets N (negative), P (positive) and Z (zero). The motor current was characterized by S (small) and L (large) fuzzy sets. Only the proportional tag (first output) was influenced by the protective mechanism, since the integral tag has slower control action dynamics. The protective mechanism was

Table 1. Rule base of FLC1.

	Speed error: e_v	Motor current: I_A	Proportional tag: U_P	Integral tag: U_I
1	Z	-	Z	Z
2	P	-	P	P
3	N	-	N	N
4	Z	S	Z	-
5	P	L	Nx	-
6	N	L	Px	-

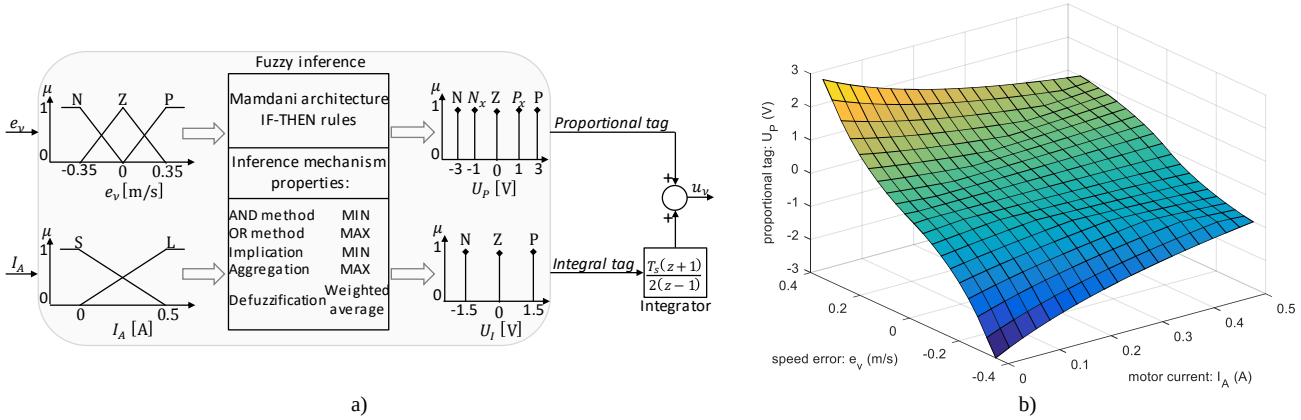

Fig. 5. (a) Structure of FLC1 and (b) the generated fuzzy surface related to the rule base.

characterized by Nx and Px fuzzy sets describing the negative and positive protective voltages, respectively. The protective nature of FLC1 is well demonstrated by its fuzzy surface depicted in Fig. 5b. It can be observed that FLC1 works as a nonlinear P controller, whose control action is decreased as the motor current increases. This nonlinearity both produces smoothness in the control and allows to reduce the current peaks and jerks in the electro-mechanical parts of the MWP.

4 Tuning of the controllers

The control structures introduced in the previous section roughly stabilizes the MWP, however, the parameters of the controllers were selected based on trial-end-error method. The trial-and-error procedure does not guarantee the best control performance, rather a compromise solution. This section describes the application of numerical optimization on the FLC parameters with the aim to maximize the control performance. The optimization algorithm results the optimal possible FLC parameters by locating the minimum of the formulated fitness function.

4.1 Parameters of the controllers

The main parameters that determine the fuzzy inference are related to the shapes and ranges of the applied membership functions. Varying the shape, position and range of these functions different control performance is achieved. The triangular membership functions and the singleton consequents can be characterized by three parameters ($p_{i,1}, p_{i,2}, p_{i,3}$ – points of the triangle) and single gains (u_i), respectively, as it was recommended in [15]. These parameters were selected to be tuned by means of numerical optimization. The initial values of these parameters are given in the fourth column of Table 2.

4.2 Fitness function

The control performance is measured with the fitness function. In [2] and [15] different formulas were recommended for the quality measurement of both the reference tracking and suppression of IB oscillations. Based on the proposed error integrals, the combination of four mean absolute errors (MAE) was chosen for the fitness function that qualifies the overall control performance. Therefore, both the quality of reference tracking (by evaluating the errors $e_\nu = \nu_d - \nu$ and $e_\xi = \xi_d - \xi$) and the efficiency of IB oscillations suppression (by evaluating the error $e_{\omega_3} = 0 - \omega_3$) as well as the average motor current (I_A) were implemented in a complex fitness function given as:

$$F = \sqrt[4]{\left(\frac{\sum|e_{\nu,j}|}{N}\right)^{\alpha}\left(\frac{\sum|e_{\omega_3,j}|}{N}\right)^{\beta}\left(\frac{\sum|e_{\xi,j}|}{N}\right)^{\gamma}\left(\frac{\sum|I_A^2|}{N}\right)^{\kappa}}, \quad (2)$$

where $j = 1 \ldots N$, N denotes the length of the measurement, while $\alpha = 1.8$, $\beta = 0.5$, $\gamma = 1.8$ and $\kappa = 0.9$ weights represent the preferences between the four control objectives. Among these weights, α and γ are the largest, since the most important quality goal is to achieve the desired planar motion as fast as possible. Moreover, the squared average motor current was considered in the formula to emphasize the effect of current peaks.

The aim of the optimization problem was to find the control parameters (p_i, d_i and u_i in Table 1 for

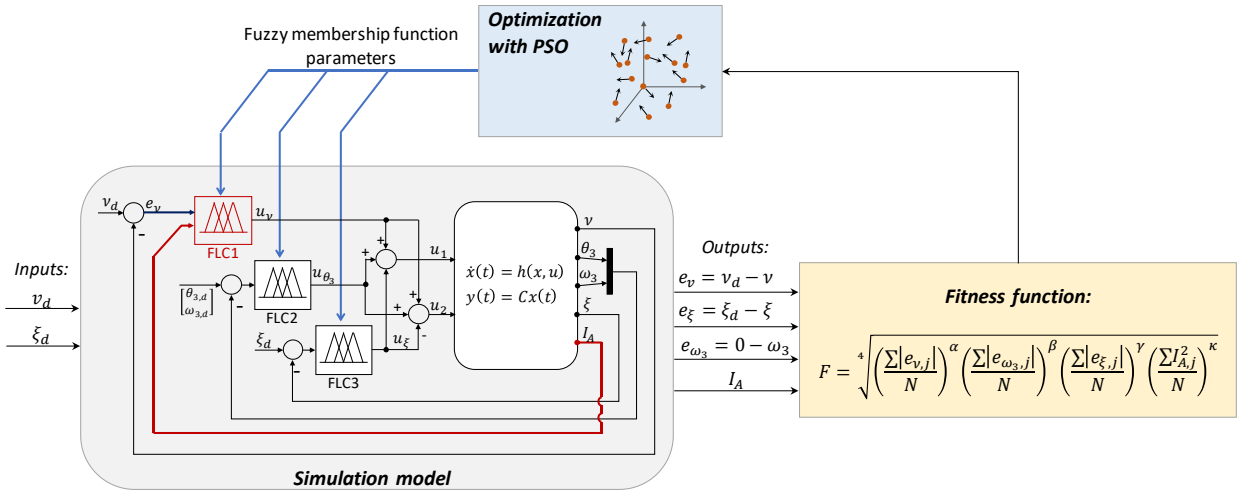

Fig. 6. Block diagram of the optimization procedure.

FLC1-3) that correspond to the minimum fitness function value.

4.3 Particle swarm optimization

The simulation environment was considered as a black box object, its inputs and outputs are the desired speeds (v_d, ξ_d) and reference tracking errors $(e_v, e_{\omega_3}, e_\xi)$ plus average motor current I_A, respectively, moreover, it is characterized by the controller parameters (see the block diagram in Fig. 6). The particle swarm optimization (PSO) was applied for the tuning of the control parameters, since it is a robust heuristic method that has already proven its fast convergence property [4].

The PSO uses an effective mechanism that mimics the swarm behavior of birds flocking and fish schooling in order to guide the particles searching for the global optimal solution in the search space. Let χ_i and δ_i denote the n-dimensional position and velocity vector of the ith particle in the swarm, while ρ_i and λ_i indicate the personal best position (which gives the best fitness value so far) of the ith particle and the neighborhood best position, respectively. The velocity and position vectors are modified in every generation based on the following equations [20]:

$$\delta_{id} = w_i\delta_{id} + c_1 r_1(\rho_{id} - \chi_{id}) + c_2 r_2(\lambda_{id} - \chi_{id}),$$
$$\chi_{id} = \chi_{id} + \delta_{id}, \tag{3}$$

where i denotes the ith particle, $d \in [1, n]$ is the dimension, c_1 and c_2 are positive constants, $r_1, r_2 \in [0,1]$ are random values, and w is the inertia weight. The parameters were selected as $w = 0.9$, $c_1 = 0.5$ and $c_2 = 1.5$ based on previously gained experiences [4], [15]. In the simulation environment the Particle swarm toolbox for MATLAB [21] was utilized. Since the fuzzy structure is characterized by 21 parameters, $n_{gen} = 210$ and $n_{pop} = 210$ were chosen for the number of generations and populations for the optimization of FLC1-3.

4.4 Results

The optimized closed loop behavior is depicted in Fig. 7, while the optimized FLC parameters are summarized in the fifth column of Table 2. The achievable maximum (linear) speed of the robot is approximately 0.5 m/s. In order to test the response time of the closed loop dynamics both fast and slow behaviors were analyzed. Therefore, the following reference (desired) signals were considered in the analysis:

- $v_d = \{0.4, 0, -0.2, 0\}$ m/sec linear speeds,
- $\xi_d = \{30, 0, -70, 0\}$ deg/sec yaw rate values.

The fitness function value (evaluating equation (2)) significantly improved after the optimization procedure, from $F_{init} = 0.1049$ (related to the initial p_i, d_i and u_i parameters in the fourth column of Table 1) to $F_{opt} = 0.0558$ providing 46.8% better overall control performance (the smaller the value the better control performance is achieved).

Based on Fig. 7 it can be observed, that the optimized FLC parameters ensure fast closed loop behavior (the reference values are achieved in less than 0.7 sec), moreover the oscillation of the IB is limited and quickly suppressed (similarly, in less than 0.7 sec). The optimization resulted an efficient

Table 2. Notation of the FLC parameters: initial and optimized values.

FLC1

Fuzzy set	Meaning	Parameters	Initial values	**Optimized values**
N (in)	negative	$\Gamma(-\infty, -p_{11}, -p_{12})$	$p_{11} = 0.35$ and $p_{12} = 0$	$p_{11} = 0.289$ and $p_{12} = 0$
Z (in)	zero	$\Gamma\big(-(p_{11} - p_{13}), 0, (p_{11} - p_{13})\big)$	$p_{13} = 0$	$p_{13} = 0.0019$
P (in)	positive	$\Gamma(p_{12}, p_{11}, \infty)$	-	-
S (in)	small	$\Gamma(-\infty, 0, d_{11})$	$d_{11} = 0.5$	$d_{11} = 0.783$
L (in)	large	$\Gamma(d_{12}, \mathrm{d}_{13}, \infty)$	$d_{12} = 0$ and $d_{13} = 0.5$	$d_{12} = 0.17$ and $d_{13} = 0.953$
N, P (U_P out)	negative and positive consequent gains (Fig. 5a)	u_{11}	$\lvert u_{11}\rvert = 3$	$\lvert u_{11}\rvert = 1.002$
N_x, P_x (U_P out)		u_{12}	$\lvert u_{12}\rvert = 1$	$\lvert u_{12}\rvert = 0.22$
N, P (U_I out)		u_{13}	$\lvert u_{13}\rvert = 1.5$	$\lvert u_{13}\rvert = 5.26$

FLC2

Fuzzy set	Meaning	Parameters	Initial values	**Optimized values**
N (in1)	negative	$\Gamma(-\infty, -p_{21}, -p_{22})$	$p_{21} = 15$ and $p_{22} = 0$	$p_{21} = 27.04$ and $p_{22} = 0$
Z (in1)	zero	$\Gamma\big(-(p_{21} - p_{23}), 0, (p_{21} - p_{23})\big)$	$p_{23} = 0$	$p_{23} = 1.122$
P (in1)	positive	$\Gamma(p_{22}, p_{21}, \infty)$	-	-
N (in2)	negative	$\Gamma(-\infty, -d_{21}, -d_{22})$	$d_{21} = 220$ and $d_{22} = 0$	$d_{21} = 657.93$ and $d_{22} = 0$
Z (in2)	zero	$\Gamma\big(-(d_{21} - d_{23}), 0, (d_{21} - d_{23})\big)$	$d_{23} = 0$	$d_{23} = 13.301$
P (in2)	positive	$\Gamma(d_{22}, d_{21}, \infty)$	-	-
NS, PS (out)	negative and positive consequent gains	u_{21}	$\lvert u_{21}\rvert = 0.6$	$\lvert u_{21}\rvert = 1.068$
NL, PL (out)		u_{22}	$\lvert u_{22}\rvert = 0.6$	$\lvert u_{22}\rvert = 0.504$

FLC3

Fuzzy set	Meaning	Parameters	Initial values	**Optimized values**
N (in)	negative	$\Gamma(-\infty, -p_{31}, -p_{32})$	$p_{31} = 30$ and $p_{32} = 0$	$p_{31} = 16.629$ and $p_{32} = 0$
Z (in)	zero	$\Gamma\big(-(p_{31} - p_{33}), 0, (p_{31} - p_{33})\big)$	$p_{33} = 0$	$p_{33} = 3.970$
P (in)	positive	$\Gamma(p_{32}, p_{31}, \infty)$	-	-
N, P (out)	neg. and pos. consequent gains	u_3	$\lvert u_3\rvert = 1.5$	$\lvert u_3\rvert = 2.398$

control structure that remarkably enhanced the system behavior (fast and effective reference tracking). Moreover, the electro-mechanical parts of the MWP are protected, since high peaks and jerks related to inner body oscillations are limited. The flexibility of the fuzzy logic controllers allowed to significantly reduce the motor current peaks. The initial closed loop dynamics was characterized by 0.5-0.6A motor current transients. These transients were limited to 0.2A current peaks by employing the optimized FLCs, therefore with smaller current consumption and limited jerks and current peaks, the electro-mechanical parts of the MWP are more protected.

Regarding the partial fitness function results, it can be remarked that the reference tracking performance was enhanced by 13% and 59% for the linear speed and yaw rate control, respectively, while the performance of the suppression of the IB oscillation was enhanced by 36% with the optimized fuzzy control structure. The protective and smooth nature of FLC1 made the mean absolute motor current to reduce from 0.035A to 0.019A.

The achieved control performance showed that both the flexibility fuzzy logic provides and the application of the effective PSO algorithm allowed to significantly enhance the overall control performance. This performance can be further improved with more sophisticated fuzzy logic controllers that are characterized by bigger rule bases and more linguistic values (e.g., the inputs and outputs of the FLCs could be decomposed into five membership functions in order to define finer and more advanced fuzzy inference machines). The investigation of more advanced FLCs is left for another paper.

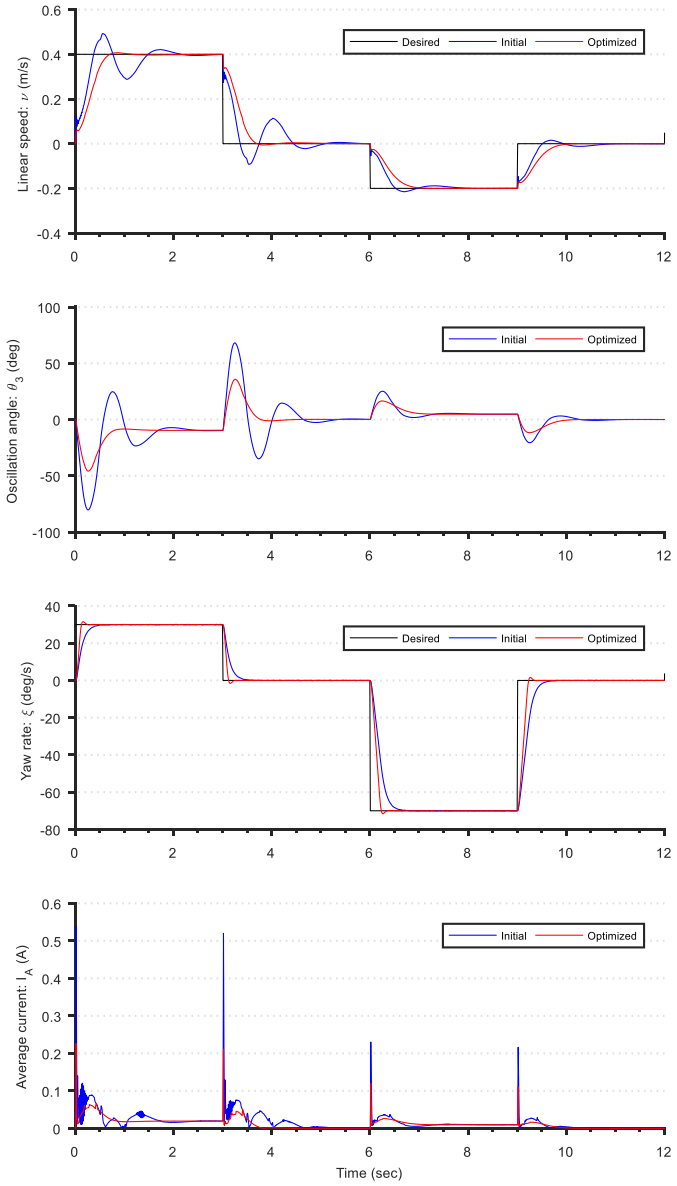

Fig. 7. Closed loop dynamics before (blue) and after (red) the optimization.

5 Implementation of the controllers

The hardware architecture of the robot is built around two MSP430F2618 microcontrollers (16bit, 16MHz, 116kB Flash, 8kB RAM) and is described in detail in [12]. The embedded software is written in C language. The control signals are calculated with floating point operations, then they are converted to PWM duty cycles. The PWM signals are transmitted to H-bridges that drive the DC motors. The developed fuzzy control structure was implemented in the first microcontroller (MCU1). First, this microcontroller collects the encoder, inertial measurement unit (IMU) and current sensor measurements, then the state vector introduced in section 2 is determined. The selected control algorithm is executed in every 10ms. The flowchart of the embedded software is depicted in Fig. 8.

The fuzzy logic controllers were approximated with look-up tables. These look-up tables (LUT) describe the fuzzy surface which plainly expresses the relationship between the crisp inputs and outputs of the FLCs. Therefore, LUT1-3 (approximations of FLC1-3) were generated by evaluating the possible input combinations and registering the corresponding control signal in a LUT for each FLC (e.g., in case of FLC1, $e_\nu = 0.2$ m/s and $I_A = 0.062$ A input combination yields $u_P = 0.53$ V control signal for the proportional tag). Consequently, each element of a LUT corresponds to certain input pairs.

The generated LUTs were stored in the flash memory of the microcontroller. The size (resolution) of each implemented LUT was 40x40, i.e., the input ranges were equidistantly divided into 40 input values. Since, the motors are driven with 10-bit resolution PWM signals stored in 16-bit integer variables, therefore the size of a LUT was $M_{LUT} \approx 3.2$kByte. This LUT based implementation method requires less calculation (compared to the method, where fuzzification, implication, and defuzzification calculations are performed), because only the table indexes are needed to be calculated. The crisp output is selected based on the table indexes. However, the precision of the control output both depends on the LUT size and the resolution of the PWM signal.

The control signal (crisp output) is calculated by searching in the table using the relevant instantaneous measurements. As an example, the row (ind_1) and column (ind_2) indexes and the crisp output (u_{θ_3}) of FLC2 are calculated as:

$$\begin{aligned} \text{ind}_1 &= \text{round}\left(e_{\theta_3} - e_{\theta_3}^{\min}\right)/\text{res}_1, \\ \text{ind}_2 &= \text{round}\left(e_{\omega_3} - e_{\omega_3}^{\min}\right)/\text{res}_2, \\ u_{\theta_3} &= \text{LUT}_2(\text{ind}_1, \text{ind}_2), \end{aligned} \tag{4}$$

where res_1 and res_2 denote the resolutions of the input ranges, while $e_{\theta_3}^{\min}$ and $e_{\omega_3}^{\min}$ indicate the least possible values of the inputs. In the fuzzy control structure, the control signals of the motors were calculated as:

$$\begin{aligned} u_{1,k} &= \text{LUT}_1|_{e_{\nu,k}} + \text{LUT}_2|_{e_{\theta_3,k}, e_{\omega_3,k}} + \text{LUT}_3|_{e_{\xi,k}}, \\ u_{2,k} &= \text{LUT}_1|_{e_{\nu,k}} + \text{LUT}_2|_{e_{\theta_3,k}, e_{\omega_3,k}} - \text{LUT}_3|_{e_{\xi,k}}. \end{aligned} \tag{5}$$

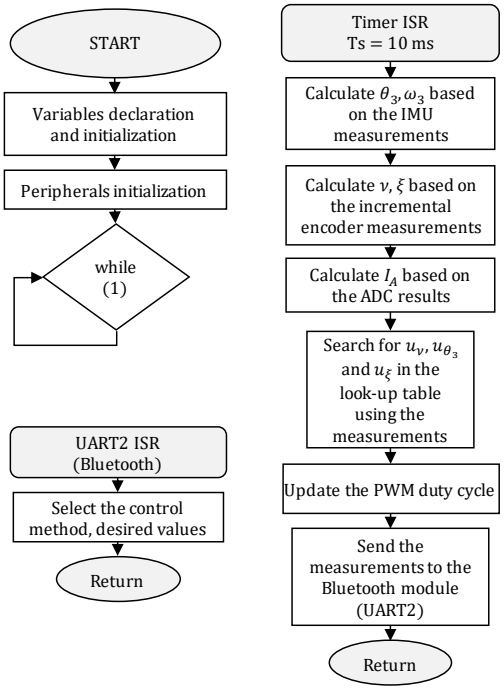

Fig. 8. Flowchart of the embedded software.

where the output signals ($u_{\nu,k}, u_{\theta_3,k}$ and $u_{\xi,k}$) are selected in LUT1-3 based on both equation (4) and the corresponding error signal ($e_{\nu,k}$, $e_{\theta_3,k}$ and $e_{\omega_3,k}$ or $e_{\xi,k}$).

6 Conclusion

This paper introduced a protective fuzzy control structure for the stabilization of a wheeled pendulum system and described the application of particle swarm optimization on FLCs to enhance the overall control performance. In the control structure, a special PI-type FLC was applied that evaluated the motor current beside the error signal. The heuristic inference mechanism allowed to produce smooth control action thereby limiting the current peaks in the motor drive system. A complex performance index was formulated that considered the reference tracking errors as well as the current consumption with certain preferences. This performance index was minimized in an optimization procedure which resulted the optimal possible FLC parameters. The achieved closed loop behavior demonstrated that the optimized fuzzy control structure enhanced the overall control performance by 46.8%. The optimized FLCs provided fast system dynamics, less inner body oscillations and smaller motor current peaks, yielding an optimized dynamical behavior that more protects the electro-mechanical structure of the MWP. Future work will involve the validation of the mathematical model of the plant and the comparison of the developed control strategies with other modern control techniques.

Acknowledgements: This publication is supported by the EFOP-3.6.1-16-2016-00003 project. The project is co-financed by the European Union. The authors would also like to thank Dr. Fritz Faulhaber GmbH & Co. KG their high precision DC micromotors that were used in the mobile pendulum system.

References:

[1] L.-X. Wang, *A course in fuzzy systems*. Prentice-Hall press, USA, 1999.

[2] Á. Odry, J. Fodor, and P. Odry, "Stabilization of a two-wheeled mobile pendulum system using LQG and fuzzy control techniques," *International Journal On Advances in Intelligent Systems*, vol. 9, no. 1,2, pp. 223–232, 2016.

[3] Á. Odry, E. Burkus, and P. Odry, "LQG control of a two-wheeled mobile pendulum system," *The Fourth International Conference on Intelligent Systems and Applications (INTELLI 2015)*, pp. 105–112, 2015.

[4] I. Kecskés and P. Odry, "Optimization of PI and fuzzy-PI controllers on simulation model of Szabad(ka)-ii walking robot," *International Journal of Advanced Robotic Systems*, vol. 11, no. 11, p. 186, 2014.

[5] J.-X. Xu, Z.-Q. Guo, and T. H. Lee, "Design and implementation of a takagi–sugeno-type fuzzy logic controller on a two-wheeled mobile robot," *IEEE Transactions on Industrial Electronics*, vol. 60, no. 12, pp. 5717–5728, 2013.

[6] C.-H. Huang, W.-J. Wang, and C.-H. Chiu, "Design and implementation of fuzzy control on a two-wheel inverted pendulum," *IEEE Transactions on Industrial Electronics*, vol. 58, no. 7, pp. 2988–3001, 2011.

[7] A. Salerno and J. Angeles, "A new family of two-wheeled mobile robots: Modeling and controllability," *IEEE Transactions on Robotics*, vol. 23, no. 1, pp. 169–173, 2007.

[8] J. Angeles, *Fundamentals of robotic mechanical systems: theory, methods, and algorithms*. Springer Science & Business Media, 2013.

[9] A. Salerno and J. Angeles, "The control of semi-autonomous two wheeled robots undergoing large payload-variations," *IEEE International Conference on Robotics and*

Automation (ICRA'04), vol. 2, pp. 1740–1745, 2004.

[10] P. Oryschuk, A. Salerno, A. M. Al-Husseini, and J. Angeles, "Experimental validation of an underactuated two-wheeled mobile robot," *IEEE/ASME Transactions on Mechatronics*, vol. 14, no. 2, pp. 252–257, 2009.

[11] B. Cazzolato, J. Harvey, C. Dyer, K. Fulton, E. Schumann, T. Zhu, Z. Prime, B. Davis, S. Hart, E. Pearce et al., "Modeling, simulation and control of an electric diwheel," in *Australasian Conference on Robotics and Automation*, pp. 1–10, 2011.

[12] Á. Odry, I. Harmati, Z. Király, and P. Odry, "Design, realization and modeling of a two-wheeled mobile pendulum system," *14th International Conference on Instrumentation, Measurement, Circuits and Systems (IMCAS '15)*, pp. 75–79, 2015.

[13] Á. Odry, E. Burkus, I. Kecskés, J. Fodor, and P. Odry, "Fuzzy control of a two-wheeled mobile pendulum system," *IEEE 11th International Symposium on Applied Computational Intelligence and Informatics (SACI)*, pp. 99–104, 2016.

[14] AppL-DSP.com: Video demonstration of the system dynamics, http://appldsp.com/lqg-and-fuzzy-control-of-a-mobile-wheeled-pendulum/, accessed 4 June 2017.

[15] Á. Odry, I. Kecskés, E. Burkus, Z. Király, and P. Odry, "Optimized Fuzzy Control of a Two-Wheeled Mobile Pendulum System," *International Journal of Control Systems and Robotics*, vol. 2, pp. 73-79, 2017.

[16] G. Carbone, "Stiffness analysis and experimental validation of robotic systems," *Frontiers of Mechanical Engineering*, vol. 6, no. 2, pp. 182-196, 2011.

[17] I. Kecskés, E. Burkus, Z. Király, Á. Odry, and P. Odry, "Competition of Motor Controllers Using a Simplified Robot Leg: PID vs Fuzzy Logic," *4th International Conference on Mathematics and Computers in Sciences and Industry (MCSI)*, 2017, in press.

[18] A. Odry, D. Toth, and T. Szakall, "Two independent front-wheel driven robot model," *IEEE 6th International Symposium on Intelligent Systems and Informatics (SISY)*, pp. 1-3, 2008.

[19] J. Basilio and S. Matos, "Design of PI and PID controllers with transient performance specification," *IEEE Transactions on education*, vol. 45, no. 4, pp. 364-370, 2002.

[20] J. F. Kennedy, J. Kennedy, R. C. Eberhart, and Y. Shi, *Swarm intelligence*. Morgan Kaufmann, 2001.

[21] psomatlab: Particle swarm toolbox for matlab, https://code.google.com/p/psomatlab/, accessed 4 June 2017.

[22] K. J. Åström and T. Hägglung, *Advanced PID control*. ISA-The Instrumentation, Systems and Automation Society, 2006.